2018

Micro-hydromechanical deep drawing of metal cups with hydraulic pressure effects

Liang Luo
University of Wollongong, ll895@uowmail.edu.au

Zhengyi Jiang
University of Wollongong, jiang@uow.edu.au

Dongbin Wei
University of Technology Sydney, dwei@uow.edu.au

Xiaogang Wang
Taiyuan University of Science and Technology

Cunlong Zhou
Taiyuan University of Science and Technology, zcunlong@163.com

See next page for additional authors

Publication Details

Luo, L., Jiang, Z., Wei, D., Wang, X., Zhou, C. & Huang, Q. (2018). Micro-hydromechanical deep drawing of metal cups with hydraulic pressure effects. Frontiers of Mechanical Engineering, 13 (1), 66-73.

Micro-hydromechanical deep drawing of metal cups with hydraulic pressure effects

Abstract
Micro-metal products have recently enjoyed high demand. In addition, metal microforming has drawn increasing attention due to its net-forming capability, batch manufacturing potential, high product quality, and relatively low equipment cost. Micro-hydromechanical deep drawing (MHDD), a typical microforming method, has been developed to take advantage of hydraulic force. With reduced dimensions, the hydraulic pressure development changes; accordingly, the lubrication condition changes from the macroscale to the microscale. A Voronoi-based finite element model is proposed in this paper to consider the change in lubrication in MHDD according to open and closed lubricant pocket theory. Simulation results agree with experimental results concerning drawing force. Changes in friction significantly affect the drawing process and the drawn cups. Moreover, defined wrinkle indexes have been shown to have a complex relationship with hydraulic pressure. High hydraulic pressure can increase the maximum drawing ratio (drawn cup height), whereas the surface finish represented by the wear is not linearly dependent on the hydraulic pressure due to the wrinkles.

Disciplines
Engineering | Science and Technology Studies

Publication Details
Luo, L., Jiang, Z., Wei, D., Wang, X., Zhou, C. & Huang, Q. (2018). Micro-hydromechanical deep drawing of metal cups with hydraulic pressure effects. Frontiers of Mechanical Engineering, 13 (1), 66-73.

Authors
Liang Luo, Zhengyi Jiang, Dongbin Wei, Xiaogang Wang, Cunlong Zhou, and Qingxue Huang

FME-17038-LL

Verso: Front. Mech. Eng. 2018

Recto: Liang LUO et al. Micro-hydromechanical deep drawing with hydraulic pressure effects

DOI: 10.1007/s11465-018-0468-z

RESEARCH ARTICLE

Liang LUO, Zhengyi JIANG, Dongbin WEI, Xiaogang WANG, Cunlong ZHOU, Qingxue HUANG

Micro-hydromechanical deep drawing of metal cups with hydraulic pressure effects

Received April 5, 2017; accepted May 19, 2017

Liang LUO, Zhengyi JIANG (✉)

School of Mechanical, Materials, Mechatronic, and Biomedical Engineering, University of Wollongong, Wollongong, NSW 2522, Australia

Email: jiang@uow.edu.au

Dongbin WEI

School of Electrical, Mechanical, and Mechatronic System, University of Technology, Sydney, NSW 2007, Australia

Zhengyi JIANG, Xiaogang WANG, Cunlong ZHOU, Qingxue HUANG

School of Materials Science and Engineering, Taiyuan University of Science and Technology, Taiyuan 030024, China

Abstract Micro-metal products have recently enjoyed high demand. In addition, metal microforming has drawn increasing attention due to its net-forming capability, batch manufacturing potential, high product quality, and relatively low equipment cost. Micro-hydromechanical deep drawing (MHDD), a typical microforming method, has been developed to take advantage of hydraulic force. With reduced dimensions, the hydraulic pressure development changes; accordingly, the lubrication condition changes from the macroscale to the microscale. A Voronoi-based finite element model is proposed in this paper to consider the change in lubrication in MHDD according to open and closed lubricant pocket theory. Simulation results agree with experimental results concerning drawing force. Changes in friction significantly affect the drawing process and the drawn cups. Moreover, defined wrinkle indexes have been shown to have a complex relationship with hydraulic pressure. High hydraulic pressure can increase the maximum drawing ratio (drawn cup height), whereas the surface finish represented by the wear is not linearly dependent on the hydraulic pressure due to the wrinkles.

Keywords micro-hydromechanical deep drawing, microforming, size effects, lubrication, Voronoi

1 Introduction

The market for micro-electro-mechanical systems has grown in the past decades and is predicted to keep growing in the coming years [1]. Micro-manufacturing technologies for silicon-based micro products have been developed and used in a wide range of industrial applications [2]. However, micro-metal products that can bear heavy loads and high working temperatures are still needed. Microforming is a potential approach to fabricating these micro-metal products with complex 3D structures. Compared with other micro-metal manufacturing technologies, microforming is more advantageous because of its net-forming capability, batch manufacturing potential, high product quality, and relatively low equipment and operator training costs [3,4].

Micro deep drawing, a typical microforming method, can produce cup- or box-like micro-metal products [5]. However, this technology has to overcome challenges related to size reduction [6–8]. The drawability of a blank in micro deep drawing is lower than that in normal-scale deep drawing due to thin blank thickness, which ranges from tens to hundreds of microns. The maximum drawing ratio also changes in the microscale. In addition, material properties change in the microscale due to the reduced size and the material size effects. Thus, the properties of drawn products, such as shape accuracy and surface finish, are greatly affected.

Micro-hydromechanical deep drawing (MHDD) has been developed to improve micro deep drawing [9]. In both micro and normal scales, hydraulic force has an impact on the stress-strain state during the drawing process. Hydraulic force also provides a pre-bulging process, which benefits drawing by enhancing the blank's strength through strain hardening. Friction and drawing are thus improved by enhanced lubrication [10,11]. However, the lubrication condition changes on the

microscale and affects the MHDD process. To explain the change in friction, the open and closed lubricant pocket theory has been developed [11].

In the current study, a Voronoi-based finite element model was developed to consider the open and closed lubricant pockets separately. MHDD simulation and experiments were conducted. Finally, the simulation and experimental results were analyzed and compared.

2 Experimental

The SUS304 sheets with a thickness of 50±2 μm were annealed at 975 °C, 1050 °C, and 1100 °C for 2 min in argon gas ambient protection. Microstructures of the annealed sheets are shown in Fig. 1, and the three groups of sheets were named "H975," "H1050," and "H1100," respectively. The material parameters for the three-parameter Barlat model were obtained from the tensile tests.

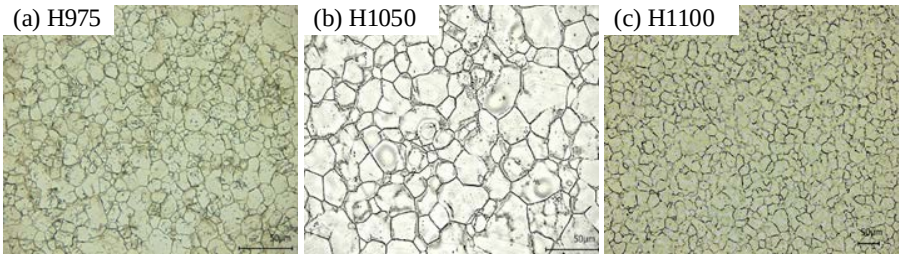

Fig. 1 Microstructures of the three groups of annealed sheets. (a) H975; (b) H1050; (c) H1100

Next, all three groups of sheets were drawn into micro cups under a series of hydraulic pressures ranging from 5–30 MPa with 5 MPa intervals (The maximum reachable hydraulic pressure in experiments was 30 MPa.). A one-step blanking-drawing process was applied in the MHDD system due to difficulties in positioning and transitioning the small blank. The drawing process continued with the blanking process, which prepared a blank in the right position. The sheets were gently cleaned by a soft eraser and then by alcohol to remove the oxidation layers and contaminants from their surfaces before the drawing experiments. After the experiments, all drawn cups were cleaned by ultrasonic bath with alcohol for 1 min and air-dried. Finally, the cleaned cups were observed under a 3D microscope, and their geometry and surface details were obtained.

3 Simulation

A normal deep drawing model with the same size as the MHDD system was initially built. The sketches of the MHDD system and the normal model are shown in Fig. 2. All parts of the model were meshed with high-quality shell elements; a blank was deformable, whereas the others were rigid. The three-parameter Barlat material model was assigned to the blank, and the surface-to-surface forming contact algorithm was used to monitor the contact and friction between the blank and the other parts. All material property parameters were obtained from the tensile experiments. A constant drawing speed of 0.1 mm/s and a fixed gap of 55 μm between the die and the blank holder were set as experimental conditions. A normal pressure load was applied on the blank.

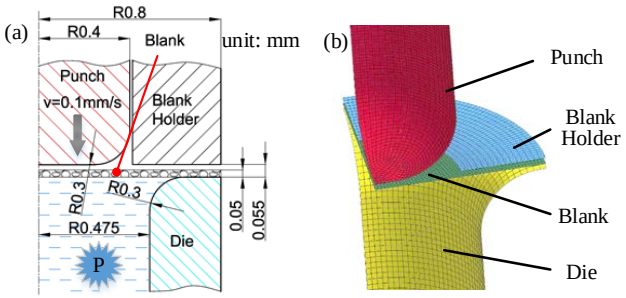

Fig. 2 (a) Sketch of the MHDD system; (b) the normal model

Centroidal Voronoi structures were utilized to consider the heterogeneous material properties on the microscale. The blank was divided into small sub-areas according to the Voronoi model, and the elements in each Voronoi cell were assigned one group of material properties. The general size of the Voronoi cell was close to the average grain size of the blank. The Voronoi models with different grain sizes are displayed in Fig. 3, in which distinct colors represent different material properties. Only five groups of material properties were used to reduce experimental work and increase simulation speed. All Voronoi cells were randomly assigned material properties.

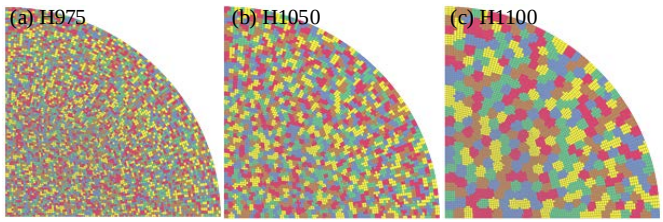

Fig. 3 Voronoi models for different blanks. (a) H975; (b) H1050; (c) H1100

According to the open and closed lubricant pocket theory, a critical radius divides a blank into open and closed lubricant pocket areas. Therefore, all Voronoi cells outside the critical radius were set as the open lubricant pocket area, and the rest comprised the closed lubricant pocket area. The open lubricant pocket area, which cannot hold the pressed lubricant, had a higher friction coefficient than the closed lubricant pocket area, which sealed the lubricant. Moreover, the critical radius decreased with the hydraulic pressure because leakage increases with hydraulic pressure. A relatively rough punch was used to improve the blank's holding capability; the friction coefficient between the blank and the punch was 0.25. The friction coefficients for each friction pair are listed in Table 1. These friction coefficient assumptions were validated by the drawing force comparison in Section 4.

The open and closed lubricant pocket models under different hydraulic pressures are shown in Fig. 4, whereas Fig. 5 presents the relationship between the hydraulic pressure and the critical radius. As can be seen, the leakage was small under low hydraulic pressures of 5–10 MPa, and only one layer of grains in the radial direction was assumed as the open lubricant pocket area. Under hydraulic pressures of 10–20 MPa, the defined open and closed lubricant pocket areas were of the same size. Under high pressures of 25–30 MPa, half of the blank's radius was set as the critical radius. Under ultra-high hydraulic pressures, the whole blank was set as the open lubricant pocket area. Given that the lubricant pocket models that were based on the Voronoi models, we consider the lubrication size effect while presenting the material size effects. Although a hydraulic pressure load was used in all the models, the friction coefficients were different in the open and closed lubricant pocket areas. Thus, the developed models well presented the lubrication size effect.

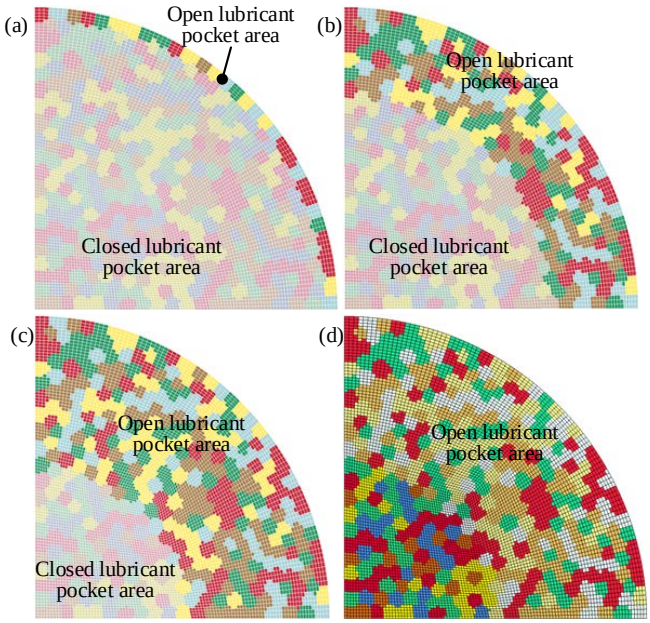

Fig. 4 The open and closed lubricant pocket models under different hydraulic pressures: (a) 5–10 MPa; (b) 15–20 MPa; (c) 25–30 MPa; (d) ultra-high hydraulic pressures

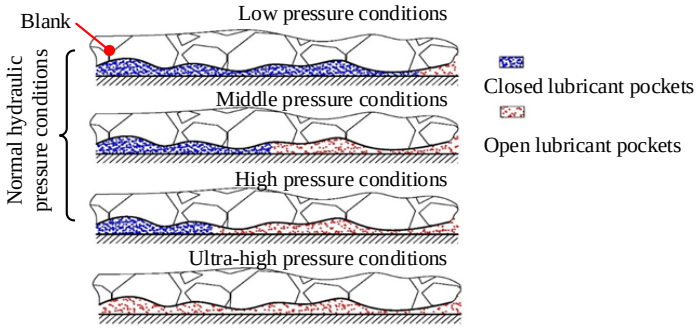

Fig. 5 Relationship between the hydraulic pressure and the critical radius

Table 1 Friction coefficients

Friction pairs	Open lubricant pocket area	Closed lubricant pocket area
Blank-die/blank-blank ~~Holder~~holder	0.10	0.05
Blank-punch	0.25	0.25

All experimental conditions were simulated by the developed models. The drawing process under ultra-high hydraulic pressures was also simulated for further prediction.

4 Results and discussion

The drawing forces between the experimental and simulation results were compared. The drawing force for H975 under 30 MPa is shown in Fig. 6. On the microscale, the friction force comprised a large part of the total drawing force and significantly affected the drawing process. The simulation results matched the experimental results well, especially in terms of the maximum drawing force, which affects drawability. The simulations of the other drawing conditions generated similar results concerning the drawing force, indicating that the general assumptions and settings (for example, friction) in the simulations were acceptable.

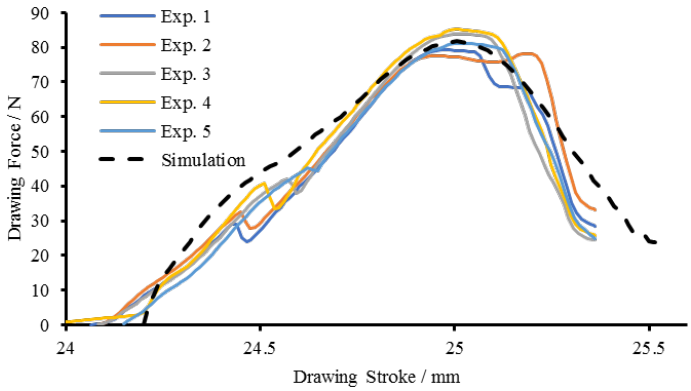

Fig. 6 Drawing forces of H975

The hydraulic pressure affected both the shape and surface finish of the drawn cups. Figure 7 shows the drawn cups with H975 sheets under different hydraulic pressures. As can be seen, the cup drawn under 30 MPa hydraulic pressure had noticeable wrinkles, whereas the cup drawn under low hydraulic pressure had a smooth mouth. Wrinkling can be prevented by the developed models due to the introduction of the Voronoi models, which presented heterogeneous blanks. A similar trend in wrinkle formation in the simulations is shown in Fig. 8.

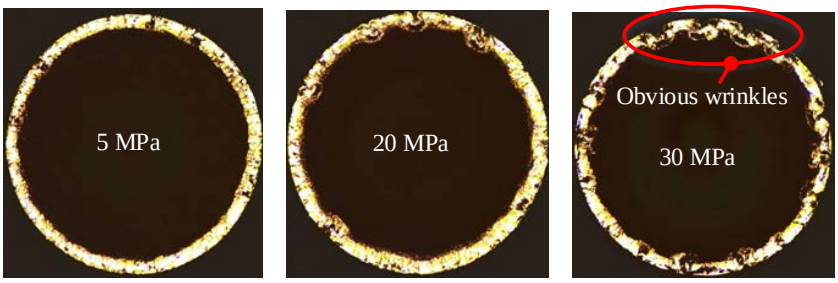

Fig. 7 Drawn cups with H975 sheets under different hydraulic pressures

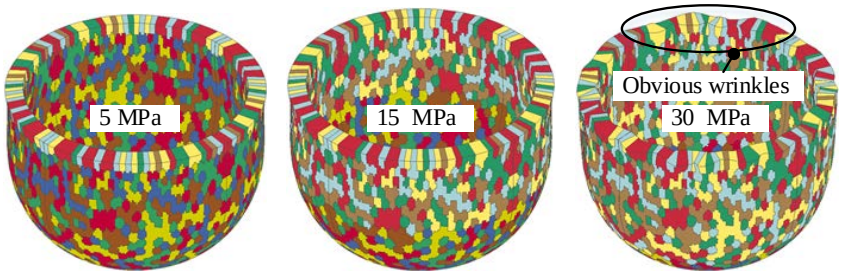

Fig. 8 Simulated drawn cups with H1100 sheets under different hydraulic pressures.

Figure 9 shows the drawn cups with different blanks under the same hydraulic pressure (30 MPa). As can be seen, the influence of the hydraulic pressure on the different blanks with different material properties changed under the same hydraulic pressure. With high strength and hardening rate, the H975 blank exhibited better resistance to wrinkling compared with the H1050 and H1100 blanks.

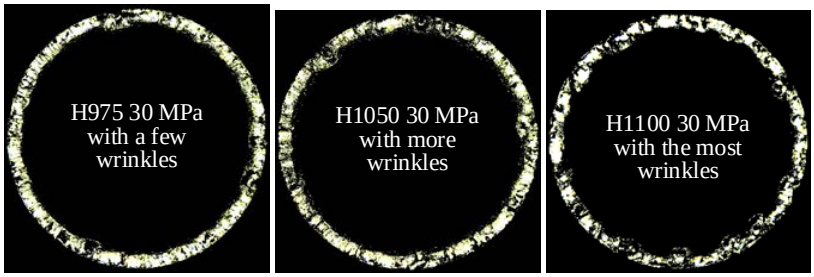

Fig. 9 Drawn cups with different blanks under 30 MPa hydraulic pressure

Similar to the surface roughness parameters R_a and R_t, two wrinkle indexes (Eqs. (2) and (3)) were defined for a quantitative analysis of the wrinkles. The position coordinates of the nodes on the drawn cup mouths were first exported and fitted against a reference circle. Next, the radial difference (Eq. (1)) between the node radius and the fitted circle radius was used for wrinkle index calculation. The equations are given by

$$r_i = R_i - R_{\text{fit}}, \quad (1)$$

$$R_t = R_p + R_v, \quad (2)$$

$$R_a = \frac{1}{N_n}\sum_{i=1}^{N_n}|r_i|, \quad (3)$$

Comment [G1]: Please explain N_n.

Comment [LL2R1]: Please see added sentence.

where r_i is the radial difference between the ith node radius R_i and fitted circle radius R_{fit}, R_t is the maximum wrinkle value, R_p is the maximum wrinkle peak height, R_v is the maximum wrinkle valley depth, ~~and~~ R_a is the average wrinkle value and N_n is the total number of nodes on cup mouth.

The defined wrinkle values were not linearly dependent on the hydraulic pressure (Fig. 10). Under 30 MPa, the maximum experimental hydraulic pressure, the defined wrinkle values gradually decrease until the hydraulic pressure was reduced to 20 MPa. These wrinkle values increased sharply over 20 MPa. Furthermore, the H1100 blank showed lower wrinkle values

than those of the other groups when the hydraulic pressure was lower than 20 MPa. By contrast, the drawn cups with the H975 blank had small wrinkle values under 30 MPa, similar to that observed in the experiments (Fig. 9).

The drawing process under ultra-high hydraulic pressures differed from that under normal hydraulic pressure conditions of 5–30 MPa. The stress and strain of the blank along the thickness direction were not fully comparable to the in-plane stress state. This stress state change significantly influenced the whole drawing process and presented wrinkle values that differed from those produced under normal hydraulic pressures. The wrinkle values under ultra-high hydraulic pressure conditions were worse than those under the best normal hydraulic pressure conditions.

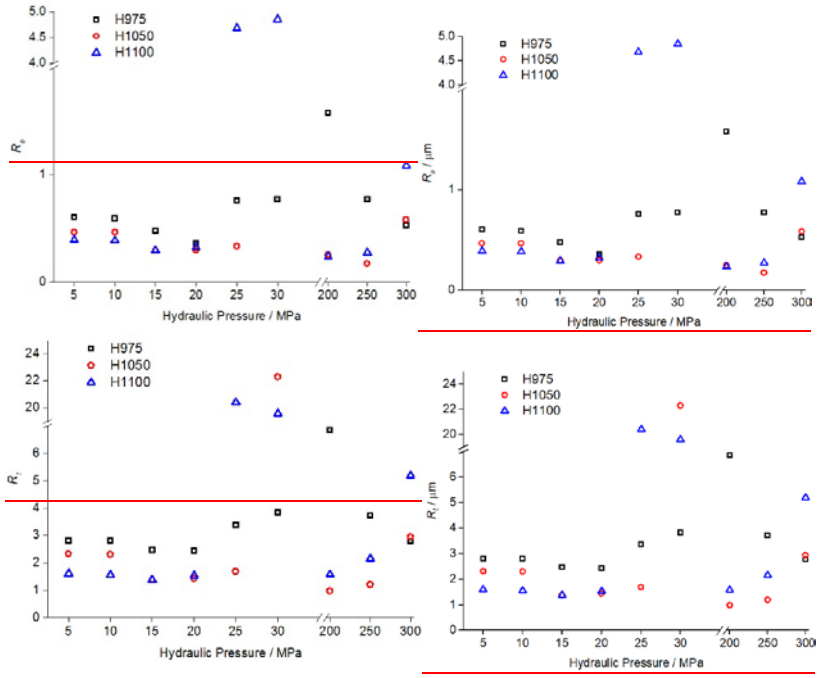

(a) wrinkle index of R_a (b) wrinkle index of R_t

Fig. 10 Wrinkle index values from simulation results (a) R_a; (b) R_t.

According to bifurcation theory based on energy analysis, wrinkles occur when the energy cost along a primary deformation path is higher than that along a secondary deformation path [12,13]. The energy consumption along the primary and secondary deformation paths in the drawing process are respectively shown in Eqs. (4) and (5):

$$E_{\mathrm{p}} = \int_{\Omega} \sigma_{ij} \Delta\varepsilon_{ij} \mathrm{d}\Omega = \int_{\Omega} \sigma_r \Delta\varepsilon_r \mathrm{d}\Omega + \int_{\Omega} \sigma_\theta \Delta\varepsilon_\theta \mathrm{d}\Omega \,, \quad (4)$$

$$E_{\mathrm{s}} = \int_{\Omega} \sigma_t \Delta\varepsilon_t \mathrm{d}\Omega + \int_{\Omega} \sigma_\theta \Delta\varepsilon_\theta \mathrm{d}\Omega \,, \quad (5)$$

where E_{p} is the energy cost along the primary deformation path, σ_{ij} is the stress in the *ij* (*ij*=*r*, *t*, θ (radial, thickness, circumferential)) directions, $\Delta\varepsilon_{ij}$ is the incremental strain in the *ij* direction, Ω is the domain of the wrinkle, and E_{s} is the energy consumption along the secondary deformation path.

The hydraulic pressure directly affected the stresses in the thickness, radial, and circumferential directions. Hydraulic pressure provided lubrication and reduced friction, thus changing the radial direction stress. The hydraulic force caused the shape of the blank to change first in the pre-bulging process, and then in the drawing process. Consequently, the circumferential direction stress also changed. The overall effects of the hydraulic pressure, material hardening, and blank deformation path resulted in a relatively complicated relationship between the wrinkle values and the hydraulic pressure.

Although the ultra-high hydraulic pressures could not significantly limit the wrinkling phenomenon, the drawing ratio (drawn cup height compared with a constant initial blank diameter) increased at the cost of reduced minimum thickness at the cup corner. As shown in Fig. 11, the cup drawn under 30 MPa had a smaller height than the cup drawn under 200 MPa. The ultra-high hydraulic pressure significantly changed the blank deformation, especially during the pre-bulging process and the first half of the drawing process. The blank was constantly in contact with the blank holder and was significantly bent in these stages. Thus, the increased friction between the blank and the blank holder provided additional radial force. Both reduced the effective die filter radius and increased friction increased the drawn cup height.

Formatted: Font: Italic

Formatted: Subscript

Formatted: Font: Italic

Formatted: Subscript

Comment [G3]: I suggest subtitles should be added for (a) and (b), respectively.
Do Ra and Rt have units?

Comment [LL4R3]: Subtitles and units were added.

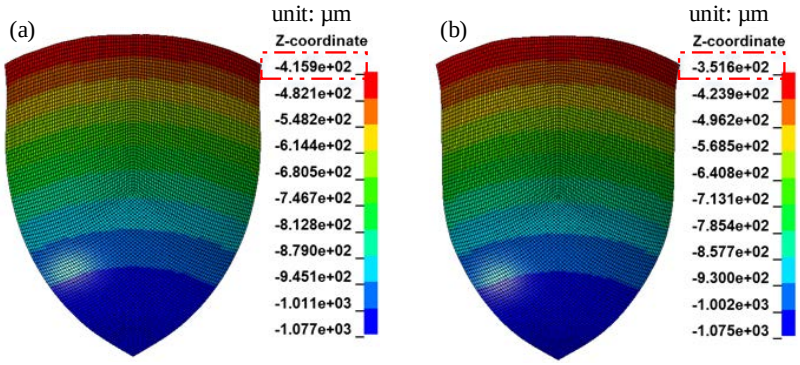

Fig. 11 Drawn cups with H975 sheets under (a) 30 MPa and (b) 200 MPa hydraulic pressures

The surface finish, deemed crucial in final products, absorbed great impact from the hydraulic pressure. High hydraulic pressures can better support the blank, and the normal contact force between the blank and the die was smaller than that under low hydraulic pressure conditions. Moreover, the hydraulic pressure changed the wrinkling phenomenon. The wrinkled area remained in contact with the die even under high hydraulic pressures, thus causing significant wear in the wrinkled area on the drawn cups. The drawn cup mouth area was the most wrinkled and therefore was the most worn. Figure 12 shows the cups drawn under different hydraulic pressures. As predicted by the defined wrinkle indexes, the cups drawn under 10 MPa had less and weaker wrinkles than those drawn under 30 MPa. The cup in Fig. 12(b) shows more wear on the cup mouth area than that drawn under 10 MPa (Fig. 12(a)).

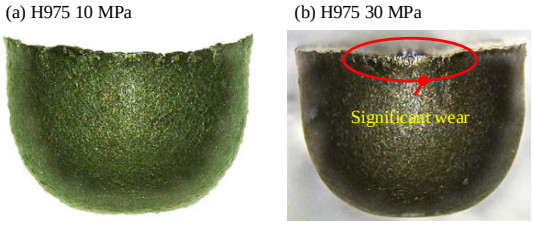

Fig. 12 Drawn cups with H975 sheets under different hydraulic pressures: (a) H975 10 MPa; (b) H975 30 MPa

The commonly used ~~*pv*~~ *PV* value (normal pressure × velocity, as shown in Eq. (6)) was used to quantitatively represent the wear during the whole drawing process

$$PV_i = \int p_i(t) \times v_i(t) dt, \quad (6)$$

where p_i and v_i ~~is~~ are the normal contact pressure~~, and v is~~ and the sliding velocity of the ith node, respectively, t is the time.

All elements on the drawn cup mouth were recorded, and the difference between the maximum and the minimum ~~*pv*~~ *PV* values was used to represent the wear of each drawn cup (Fig. 13). A high ~~*pv*~~ *PV* value difference indicates a significant difference in contact between the blank and the die as well as the wrinkles. Results showed that ultra-high hydraulic pressures resulted in a high ~~*pv*~~ *PV* value difference, which decreased when the hydraulic pressure gradually increased to 30 MPa. Meanwhile, the hydraulic force supported the blank and reduced friction or wear under hydraulic pressures lower than 30 MPa. By contrast, wrinkles introduced significant contact and noticeably increased wear, although the high hydraulic pressure effectively supported the blank. The significant wear consequently reduced the wrinkles and resulted in relatively low wrinkle values under ultra-high hydraulic pressure drawing conditions

Comment [G5]: Please check this equation.
The general integral formula is $F(x) = \int f(x) dx$.

Comment [LL6R5]: Please see revised equation

Formatted: Subscript

Formatted: Font: Italic

Formatted: Font: Times New Roman

Formatted: Font: Times New Roman, Italic

Formatted: Font: Times New Roman

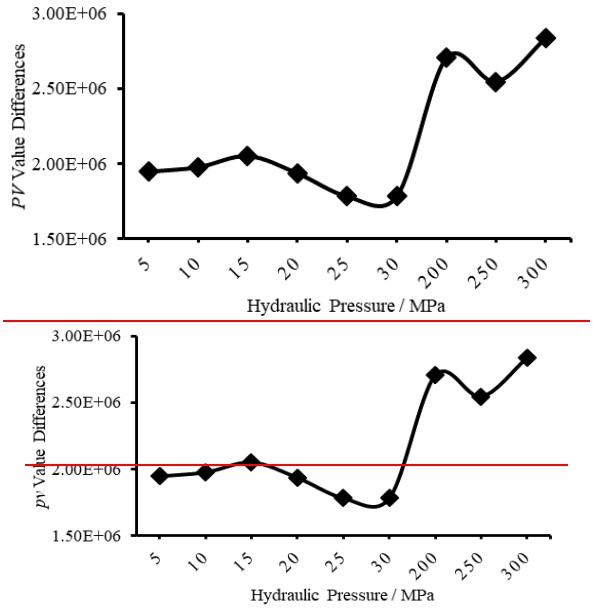

Fig. 13 The ~~*pv*~~ *PV* value differences of the drawing process with H975 sheets

Although the models successfully predicted the MHDD process by considering the material and lubrication size effects, shell elements based on in-plane stress assumption were not fully suitable for 3D deformation simulation, such as in the case of simulation with ultra-high hydraulic pressures. Solid elements can be introduced to obtain more accurate simulation results. Additionally, the hydraulic pressure was assumed to be uniformly distributed on the blank and constant during the whole drawing process, which was not the case in the experiments. Strong fluid-solid interaction can also be introduced to accurately consider the hydraulic pressure effects and the hydraulic pressure distribution on the blank.

5 Conclusions

The developed Voronoi model effectively present the heterogeneity of the blank on the microscale, and the open and closed lubricant pocket models based on the Voronoi model can consider the hydraulic pressure effects. The wrinkling phenomenon can, therefore, be presented and its complex relationship with the hydraulic pressure can be reflected by the developed models.

On the microscale, friction is significant in the drawing process, and the friction conditions differ. The wrinkling can be predicted by bifurcation theory according to the energy consumption, which is significantly affected by friction. Although ultra-high hydraulic pressure cannot restrict the wrinkling, it increases the maximum drawing ratio with the increase in drawn cup height. Additionally, the high pressure can support the blank and separate the blank and the die, thereby improving the surface finish of the drawn cups. However, the wrinkled area causes heavy contact between the blank and the die, which results in significant wear on the cups.

Acknowledgements The first author is grateful for the financial support given by the Chinese Scholarship Council (CSC 201206160011) and for the international postgraduate tuition award offered by the University of Wollongong. The authors would also like to thank the Australian Research Council for their financial support. This study was also supported by the invitation fellowship program of the Japan Society for the Promotion of Science (Z. Y. Jiang).

References

1. Goel P. MEMS non-silicon fabrication technologies. Sensors and Transducers, 2012, 139(4): 1–23 doi:10.1605/01.301-0019658108.2012

2. Huff M. MEMS fabrication. Sensor Review, 2002, 22(1): 18–33 doi:10.1108/02602280210697087

3. Geiger M, Kleiner M, Eckstein R, et al. Microforming. CIRP Annals—Manufacturing Technology, 2001, 50(2): 445–462 doi:10.1016/S0007-8506(07)62991-6

4. Tiesler N, Engel U. Microforming—Effects of miniaturization. In: Proceeding of the 8th International Conference on Metal Forming. Rotterdam: A.A.Balkema, 2000, 355–360 ISBN: 90 5809 157 0

5. Vollertsen F, Hu Z, Niehoff H S, et al. State of the art in micro forming and investigations into micro deep drawing. Journal of Materials Processing Technology, 2004, 151(1–3): 70–79 doi:10.1016/j.jmatprotec.2004.04.266

6. Deng J H, Fu M W, Chan W L. Size effect on material surface deformation behavior in micro-forming process. Materials Science and Engineering: A, 2011, 528(13–14): 4799–4806 doi:10.1016/j.msea.2011.03.005

7. Molotnikov A, Lapovok R, Gu C F, et al. Size effects in micro cup drawing. Materials Science and Engineering: A, 2012, 550: 312–319 doi:10.1016/j.msea.2012.04.079

8. Vollertsen F. Size effects in micro forming. Key Engineering Materials, 2011, 473: 3–12

9. Sato H, Manabe K, Furushima T, et al. On the scale dependence of micro hydromechanical deep drawing. Key Engineering Materials, 2017, 725: 689–694

10. Wang C, Guo B, Shan D, et al. Tribological behaviors in microforming considering microscopically trapped lubricant at contact interface. International Journal of Advanced Manufacturing Technology, 2014, 71(9–12): 2083–2090 doi:10.1007/s00170-014-5657-2

11. Sato H, Manabe K, Wei D, et al. Tribological behavior in micro-sheet hydroforming. Tribology International, 2016, 97: 302–312 doi:10.1016/j.triboint.2016.01.041

12. Wang X, Cao J. On the prediction of side-wall wrinkling in sheet metal forming processes. International Journal of Mechanical Sciences, 2000, 42(12): 2369–2394 doi:10.1016/S0020-7403(99)00078-8

13. Wang X, Cao J. An analytical prediction of flange wrinkling in sheet metal forming. Journal of Manufacturing Processes, 2000, 2(2): 100–107 doi:10.1016/S1526-6125(00)70017-X